NATIONAL AERONAUTICS AND SPACE ADMINISTRATION

SPACE SHUTTLE

AEROTHERMODYNAMIC DATA REPORT

JOHNSON SPACE CENTER

HOUSTON, TEXAS

DATA MANagement services

SPACE DIVISION CHRYSLER CORPORATION

March 1977

DMS-DR-2363
NASA CR-151,057

RESULTS OF FLUTTER TEST OS7 OBTAINED USING THE 0.14-SCALE SPACE SHUTTLE ORBITER FIN/RUDDER MODEL NUMBER 55-0 IN THE NASA LaRC 16-FOOT TRANSONIC DYNAMICS WIND TUNNEL

by

C. L. Berthold
Shuttle Aero Sciences
Rockwell International Space Division

Prepared under NASA Contract Number NAS9-13247

by

Data Management Services
Chrysler Corporation Michoud Defense-Space Division
New Orleans, La. 70189

for

Engineering Analysis Division

Johnson Space Center
National Aeronautics and Space Administration
Houston, Texas

WIND TUNNEL TEST SPECIFICS:

Test Number:	LaRC TDT 246
NASA Series Number:	OS7
Model Number:	55-0
Test Dates:	August 14 through August 30, 1974
Occupancy Hours:	88

FACILITY COORDINATOR:

B. Spencer, Jr.
Mail Stop 365
Langley Research Center
Langley Station
Hampton, VA 23665

Phone: (804) 827-3911

PROJECT ENGINEERS:

C. L. Berthold
Mail Code AD38
Rockwell International
Space Division
12214 Lakewood Boulevard
Downey, CA 90241

Phone: (213) 922-4620

F. Rauch
G. Commerford
T. Foley
Grumman Aerospace Corporation
Bethpage, New York 11714

Phone(713) 488-5660

DATA MANAGEMENT SERVICES:

Prepared by: Liaison-- D. A. Sarver
Operations--Maurice Moser, Jr.

Reviewed by: G. G. McDonald

Approved: _____ Concurrence: _____
J. L. Glynn, Manager
Data Operations

N. D. Kemp, Manager
Data Management Services

RESULTS OF FLUTTER TEST OS7 OBTAINED USING THE 0.14-SCALE SPACE SHUTTLE ORBITER FIN/RUDDER MODEL NUMBER 55-0 IN THE NASA LaRC 16-FOOT TRANSONIC DYNAMICS WIND TUNNEL

by

C. L. Berthold, Rockwell International Space Division

ABSTRACT

A 0.14-scale dynamically scaled model of the space shuttle orbiter vertical tail was tested in the Langley Research Center 16-Foot Transonic Dynamics Wind Tunnel during August 1974 to determine flutter, buffet, and rudder buzz boundaries. Mach numbers between .5 and 1.11 were investigated. Rockwell shuttle model 55-0 was used for this investigation. A description of the test procedure, hardware, and results of this test is presented herein.

(THIS PAGE INTENTIONALLY LEFT BLANK.)

TABLE OF CONTENTS

INDEX OF FIGURES

INTRODUCTION

Flutter boundaries for the space shuttle orbiter configuration 140B vertical tail were investigated. This investigation was conducted in the NASA Langley Research Center's 16-Foot Transonic Dynamics Wind Tunnel. The model was a 0.14-scale dynamically scaled vertical panel mounted on a rigid model of a segment of the orbiter upper aft fuselage. This investigation was called OS7. The model was designed and fabricated by Grumman Aerospace Corporation (GAC) under purchase order agreement M3W3XMU483002 with Rockwell International Corporation's Space Division. Grumman also performed pretest measurements and calibrations of the model, conducted the test, and analyzed the test results under this same purchase order. Much of the information presented in this report was derived from Reference 1, which is Grumman's final document of its work under this purchase order.

NOMENCLATURE

SYMBOL	DEFINITION
a_r	ratio of flight vehicle to model speed of sound
CG	center of gravity
EI	bending stiffness, slug-ft^3/sec^2
f	measured frequency of oscillation, H_z
F_n	Froude number
g_r	gravitational acceleration ratio
GJ	torsional stiffness, slug-ft^3/sec^2
H_o	freestream total pressure, psf
I_o	calculated moment of inertia plus tare inertia of model rig, lb.-in^2
$I_{X'_{CG}}$	inertia about X' axis with origin at the center of gravity, lb-in^2
$I_{Y'_{CG}}$	inertia about Y' axis with origin at the center of gravity, lb-in^2
$I_{Z'_{CG}}$	inertia about Z' axis with origin at the center of gravity, lb-in^2
k	reduced frequency
k_r	ratio of flight vehicle to model reduced frequency
K	spring rotational rate, in-lb/radian
ℓ	geometric reference length, ft
L	length dimension
m	mass, slugs
m_r	ratio of flight vehicle to model mass
M	mass dimension, Mach number

NOMENCLATURE (Continued)

SYMBOL	DEFINITION
M_∞	freestream Mach number
P_y	load in y direction
q_∞	freestream dynamic pressure, psf
R_n	Reynolds number
T	time, sec
T_Z	torsion about Z - axis, ft-lb
v	air speed, ft/sec
W	weight, lb
X_o	orbiter longitudinal coordinate, in
X'_o	vertical tail coordinate perpendicular to 50% chord line, in
X'_{CG}	X' dimension of center of gravity, in
Y_o	orbiter lateral coordinate, in
Y'	vertical tail coordinate parallel to 50% chord line, in
Y'_{CG}	Y' dimension of center of gravity, in
Z_o	orbiter vertical coordinate, in
Z'	vertical tail coordinate orthogonal to vertical tail reference plane, in
Z'_{CG}	Z' of center of gravity
δ_y	deflection in y direction
θ_Z	angular deflection about Z axis, radians
μ_r	ratio of model to flight vehicle absolute viscosity coefficients
H_t	constant total pressure

NOMENCLATURE (Concluded)

SYMBOL	DEFINITION
ρ	freestream air density, slugs/ft^3
ω	frequency, h_z
H_L	hinge line
$\mathbb{C}_t$	center line
SUBSCRIPTS	
a/c	full scale flight vehicle value
model	model value
r	ratio of model to flight vehicle
X	value referenced to X - axis
X'	value referenced to X' - axis
Y	value reference to Y - axis
Y'	value referenced to Y' - axis
Z	value referenced to Z - axis
Z'	value referenced to Z' - axis

CONFIGURATIONS INVESTIGATED

The number 55-0 fin-rudder model was a 0.140 geometric scale representation of 140B space shuttle orbiter components. It was dynamically scaled; i.e., the reduced frequency ratio and mass density ratio were scaled to 1.0 to properly simulate stiffness and mass properties of the full scale structures. The model scale factors were established to assure that estimated flutter boundaries fell within the range of the LaRC 16-foot TDT. The model had a stressed skin design constructed of epoxy-resin (pre-preg) fiberglass plies layed up on cellular-cellulose acetate (CCA) foam backing; local areas such as root attachments and actuator back-up structure were reinforced by steel sheet (.003" thick) to assure a smooth load transition at the metal-fiberglass interfaces. The model had a control surface rudder with actuator stiffnesses modeled by steel flexural pivots. Access panels at the control surface actuator locations facilitated changing the pivot flexures. Different flexures were tested to simulate nominal, 75% of nominal, and 50% of nominal actuator stiffnesses. Fuselage fairings adjacent to the fin were size scaled to simulate proper local flow characteristics as well as to place the surface outside the tunnel boundary layer; they were not dynamically scaled. The fairings were constructed of fiberglass skin attached to aluminum frames. The model consisted of the following components:

1. One sidewall mount to tunnel mounting plate
2. One partial non-dynamic fuselage

3. One vertical fin assembly (including rudder)
4. One additional set of rudders (upper and lower)
5. Nine rudder flexure sets
   (a) 3 Stiffness level 1
   (b) 3 Stiffness level 2
   (c) 3 Stiffness level 3
6. One internal model shaker
7. One control surface deflect/release mechanism per rudder
8. Eight (8) strain gage circuits (4 bending, 4 torsion)
9. Two magnetic induction coil rudder position indicators
10. One accelerometer (vertical fin tip)
11. Control panel for shaker and deflector release mechanism

Note that Items 6 through 10 and one (1) set of Item 5 were included as part of Item 3. Figure 1 shows the model assembly. Figure 2 shows the rib arrangement. Figure 3 presents photographs of the model.

The following scaling parameters were used to simulate an altitude of 30,000 feet during the test:

Scale Factors (Model/Aircraft)

Parameter	Symbol	Dimensions	Equation	Value
Length	ℓ	L	$\ell_r=\ell_{model}/\ell_{a/c}$	.14
Air Density	ρ	ML^{-3}	$\rho_r=\rho_{model}/\rho_{a/c}$	1.07
Air Speed	v	LT^{-1}	$v_r=v_{model}/v_{a/c}$	.52
Dynamic Pressure	q	$ML^{-1}T^{-2}$	$\rho_r v^2_r$	.292

CONFIGURATIONS INVESTIGATED (Continued)

Parameter	Symbol	Dimensions	Equation	Value
Frequency	ω	T^{-1}	$k_r v_r / \ell_r / \mu_r$	3.73
Velocity		LT^{-1}	$k_r v_r$	.52
Acceleration		LT^{-2}	$k_r^2 v_r^2 / \ell_r$	1.95
Mass	m	M	$\mu_r \rho_r \ell_r^3$	2.93×10^{-3}
Mass Unbalance		ML	$\mu_r \rho_r \ell_r^4$	4.11×10^{-4}
Mass Moment of Inertia		ML^2	$\mu_r \rho_r \ell_r^5$	5.75×10^{-5}
Stiffness	EI,GJ	ML^3T^{-2}	$k_r^2 v_r^2 \rho_r \ell_r^4$	1.11×10^{-4}
Bending Spring Constant		MT^{-2}	$k_r^2 v_r^2 \rho_r \ell_r$	4.09×10^{-2}
Torsional Spring Constant		ML^2T^{-2}	$k_r^2 v_r^2 \rho_r \ell_r^3$	8.01×10^{-4}
Force		MLT^{-2}	$k_r^2 v_r^2 \rho_r \ell_r^2$	5.72×10^{-3}
Moment		ML^2T^{-2}	$k_r^2 v_r^2 \rho_r \ell_r^3$	8.01×10^{-4}
Mass Density Ratio	μ	-----	$\mu_r = m_r / \rho_r \ell_r^3$	1.0
Reduced Frequency	k	-----	$k_r = \ell_r \omega_r / v_r$	1.0
Froude Number	F_n	-----	$k_r^2 v_r^2 / \ell_r g_r$	1.93
Reynolds Number	R_n	-----	$\rho_r v_r \ell_r / \mu_r^*$	.087
Mach Number	M	-----	v_r / a_r	1.0

where: μ_r^* = absolute viscosity coefficient ratio = .90

g_r = gravitational acceleration ratio = 1.0

a_r = sonic speed ratio = .52

Air speed is the aircraft flight speed; velocity is the speed associated with vibrations of the model. These quantities differ only when the reduced frequency ratio is not unity.

Nomenclature used to designate the model components was as follows:

B_{26}	Body	Similar to B_{26} lines in area of vertical tail above W.P. 458 and with a truncated forward fuselage section.
M_7	OMS Pods	Upper portion, both pods.
V_8	Vertical Tail - 140C/D Configuration.	
R5	Rudders	Upper and Lower, 140 C/D Configuration.

A complete description of model components and dimensional data is given in Table II. The model was referred to as Configuration 1, 2, 3 or 4 depending on which flexures were used for the rudder. Table III defines these configurations.

The model was equipped with its own internal shaker and control surface deflector/release mechanism; this device was remotely activated in the tunnel control room by a GAC-supplied control box. The shakers were of the rotary unbalanced force-type driven by a flexible cable shaft and designed to produce an approximately constant force output (1.5 to 2 lbs.) from 15 to 70 Hz. The model control surface deflector/release mechanism consisted of a roller cam mounted on a pivot arm attached to the aft face of the main surface rear spar, which contacted a pawl attached to the front face of the control surface front spar. To deflect and release, i.e., "pluck" the control surface, the pivot arm was rotated via an attached cable until the roller cam contacted the pawl, forcing it aside. This action deflected the control surface until the cam overrode the pawl, releasing the control surface.

CONFIGURATIONS INVESTIGATED (Concluded)

The model had the following instrumentation:

Type of Measurement	Device Used
Uncalib. fin bending moment	Four active arm strain gage circuits
Uncalib. fin torsion	↓
Uncalib. fin bending moment	
Uncalib. fin torsion	
Uncalib. dynamic rudder position (lower)	Magnet and coil assembly
Uncalib. dynamic rudder position (upper)	Magnet and coil assembly
Fin tip acceleration	Endevco 2264 accelerometer
Lower rudder hinge moment	Tension link
Upper rudder hinge moment	Tension link
Excitation frequency	Motor tachometer

Figure 4 diagrams the instrumentation hookup and arrangement.

TEST FACILITY DESCRIPTION

Major elements of the NASA Langley Transonic Dynamics Tunnel are an electric motor drive system, a cooling system, a gas-handling system, a tunnel control room and observation chamber, a transonic test section, and a model calibration laboratory.

Test section is 16 feet square and has a uniform flow region more than 10 feet in length. Throughout this region, Mach number deviation is less than $\pm$ .005 for subsonic speeds and generally less than $\pm$ .01 above Mach 1. Maximum Mach number is 1.20. Mach number, which depends on compression ratio across the fan, is controlled by varying the motor rpm or remotely varying the angle of pre-rotation located ahead of the fan.

Transonic flow is generated by three slots in both the ceiling and floor of the test section.

Drive system consists of a two-speed range wound-rotor induction motor directly connected to a fan which may be considered as a single-stage compressor. Fan speed ranges are 24 to 235 rpm for operation in Freon-12 and 15 to 470 rpm for operation in air.

Motor speed is automatically controlled by a liquid rheostat and eddy current brake to better than $\pm$ ¼ percent. At the maximum rpm in each speed range, shaft output is 20,000 horsepower, continuous rating.

Cooling system consists of a two-row vertical tube cooler through which water is circulated to maintain a stagnation temperature under 150°F.

TEST PROCEDURE

Various calibrations and measurements were performed on the model prior to the test to determine its dynamic properties. These are described below.

Flexibility influence coefficients were measured and compared to the scaled full scale coefficients. The influence coefficients were measured as the deformation slopes (spanwise and chordwise) per unit load due to force loads singly applied to the models at prescribed locations. The slopes were measured with small mirrors attached parallel to a model surface at prescribed locations. The mirrors reflected a projected grid network onto a vertically oriented screen; any change in the angular position (slope) of a mirror due to a change in loading was detected and measured on the screen. For these measurements, the vertically oriented models were cantilevered from their respective root attachment fittings, which simulated fuselage flexibility, and the loads were applied with weight and pulley arrangements. Separate measurements of the model root attachment fitting flexibilities were made with the respective model detached; the influence coefficients (flexibilities) were the root attachment spring displacements per unit load at the point of load application. Again, the loads were applied with weights, but the linear displacements (Y and Z directions) were measured with a linear differential transformer. Resulting fin root flexibilities are presented in Table IV. Resulting bending and torsional flexibility is presented in Figures 2 and 3.

Model mass distribution was also scaled in addition to stiffness scaling for complete model dynamic simulation. To demonstrate compliance with the required model mass distribution, the following inertial properties of the model were measured:

1. weights of main surfaces and control surfaces
2. C.G. locations of the main and control surface structures
3. moments of inertia of the main surfaces about their C.G. X, Y, and Z axes
4. hinge line inertias for the control surfaces
5. C.G. moments of inertia of complete models about the pitch (Y) axis for the wing and yaw (Z) axis for the fin

The center of gravity of each model component (main end control surfaces) was located by suspending the model alternately at several (at least two) pivot points, scribing the plumb lines from the pivot points on the model surface, and thereby determining the C.G. as the intersection of these lines. Model moments of inertia were measured with the aid of a low frequency vibration rig, which was essentially an oversized flexural pivot, or a bifilar pendulum, depending on the reference axis. When using the vibration rig, the model was cantilevered normal to one of the flexural pads and caused to oscillate freely about the flexural axis. The frequency of oscillation was measured with an accelerometer mounted on the moving flexural pad. The moment of inertia of the model and the tare inertia of the rig about its flexural axis was determined from the following relationship:

$I_o = K/(2\pi f)^2$, where:

K was the measured rotational spring rate of the rig about its flexural axis (inch pounds/radian)

f was the measured frequency of oscillation (Hz), and

I_o was the calculated moment of inertia of the model plus the tare inertia of the rig about its flexural axis.

It was a simple matter to subtract the known tare inertia of the rig from the calculated inertia I_o and transfer the resultant model inertia about the flexural axis to the model's C.G. axis to obtain the model C.G. moment of inertia. The yaw axis moment of inertia was measured using a bifilar pendulum to measure oscillatory frequencies instead of the vibration rig because of model mounting constraints.

These calculations were done on a panel by panel basis, with panels as shown on Figure 1. Resulting calculations and measurements are given in Table V.

Measured model modes and frequencies were compared to calculated full-scale modes and frequencies (assuming correct model/full scale weight ratio). Ground vibration surveys were conducted on the model cantilevered from its fuselage root attachment springs. The model was instrumented with one fixed and one survey (movable) accelerometer (Endevco - Model 2264-150). Vibration excitation was provided by an electromechanical shaker with a lightweight movable element secured to the model (Miller Model-A6466). During the vibration survey, while

monitoring the response of the fixed reference accelerometer on an oscilloscope, a frequency sweep was made and the large amplitude resonant responses were noted for the first five modes of each model. Then returning to the first noted resonant response and dwelling there, a survey of the structural response was made with the portable accelerometer moved to prescribed locations on the model for each mode. Generalized mass of the modes was determined experimentally by the procedure outlined in Reference 2 and is presented in Table VI. Additional sets were measured during the test period. These measurements were made utilizing a hand held probe for data acquisition and a Goodman electromagnetic shaker for excitation. Results of these measurements are documented in Reference 1.

The model was proof-loaded to ensure that it possessed adequate strength to sustain the inertial and aerodynamic loads acting on them during the wind tunnel testing. The proof loads were based on a load estimate schedule prescribed by Rockwell International. The model test loading was achieved by placing lead sheets on the model's surface to yield equivalent shear loads and bending moments at the roots.

The model was mounted in the Langley Research Center 16-Foot Transonic Dynamics Tunnel cantilevered off the east side wall with the fuselage fairing and root attachment fitting. Within the model fuselage fairing was a rigid framed support structure which also acted as a mounting butt for the model on its root attachment fitting; the structure

was bolted to the tunnel sidewall turntable; this turntable varied the model angle of sideslip. The shaker flexible drive cable, control surface deflector/release cable, strain gage, control surface coil, accelerometer and force link wiring were routed from the semi-span mount to the control room via stainless steel tubing. Figure 1 shows a sketch of the installed model. Figure 3 presents photographs of the installed model.

The general operating procedure was to make progressively higher constant total pressure sweeps through the Mach range from 0.6 to 1.2 until the ascent trajectory plus the required 32% margin of safety was investigated. Following this, testing continued at more extreme operating conditions until flutter was obtained or tunnel operating limits were reached. Pauses were made at several discrete Mach numbers during each sweep to stabilize tunnel conditions. At these points, the main model surfaces and control surfaces were excited, respectively, by the internally mounted rotary unbalanced shaker and control surface deflect/release mechanisms. During shaker excitation, the measured model amplitudes and frequencies were recorded and interpreted to assist in predicting the onset of flutter. After the shaker excitation, each control surface was deflected and released in an attempt to initiate "buzz." During the deflect/release operation, the control surface hinge moments were measured in an attempt to predict the onset of "buzz." This procedure occurred as follows:

TEST PROCEDURE (Concluded)

1. The model was installed and visually inspected in the tunnel;

2. Modal frequencies were checked with the aid of an electro-mechanical shaker and the model instrumentation;

3. The desired tunnel operating path was selected;

4. The wind-off data readouts were recorded;

5. The wind tunnel was started and model was trimmed to zero lift during the first low q run;

6. Desired Mach number and dynamic pressure were obtained;

7. When flow conditions stabilized, the model shaker was operated at a constant sweep rate from 15-70 H_z. At the conclusion of the sweep, a review of the data was made (plots of 1/modal amplitude and modal frequency vs. q were made and used to predict the onset of flutter);

8. If no flutter was observed during step 7, the control surfaces were "plucked" one at a time in an attempt to initiate control surface "buzz"; during this "plucking" operation, a record was made of the control surface hinge moment via the force link in the actuator cable of the plucker device;

9. If no flutter was observed during step 8, a higher Mach number and q on the same constant total pressure path was used to repeat steps 7 and 8;

10. Steps 4 through 9 were repeated for different values of constant total pressure (H) until the Orbiter ascent trajectory boundary was cleared and/or the flutter boundary defined in the transonic flight regime;

11. Steps 2 - 10 were repeated for each new control surface configuration.

Two high speed movie cameras and a T.V. monitor were used during the runs to record dynamic instability. The movie cameras were located to provide both a side view and rear view of the model.

Table I summarizes the test program and tunnel conditions.

DATA REDUCTION

Freestream data were measured and reduced using standard test facility techniques. Model data recorded were:

1. Oscillograph traces of the model strain gage circuits.
2. Oscillograph traces of tunnel parameters.
3. High speed movies.
4. Tabulated data.

Figures 8 through 18 present plots of the test results.

DISCUSSION OF RESULTS

During model design, the full scale fin underwent a structural design change. Since an up-to-date fin design would not have been finalized sufficiently to permit a re-design and fabrication of the model within scheduling constraints, instructions to continue modeling to the existing design were received. The reasoning behind this was that although differences between the model and the final fin design would exist, sufficient similarities would remain to enable acquisition of valuable trend data from the model. To investigate these trends, a total of four configurations was investigated during the fin program. These configurations were used to study the effects on the dynamic characteristics of the fin due to a variation in the stiffness of the flexures used to simulate the rudder actuators. Table III outlines a description of the various configurations tested and a summary of the frequencies measured on those configurations with the model installed in the tunnel.

Configuration No. 1 was established as a base case having the nominal actuator stiffness of the obsolete fin design. Runs 1 through 14 and 21, 29 and 30 were used to test the model in this configuration. During these runs a region of buffet was uncovered roughly between Mach numbers .89 and .93. In addition to this buffet region, mild flutter was encountered during runs 5 and 7 through 14. However, this flutter was later defined, by viewing high speed movies, as an instability of the model rudder hinge hatch. This model problem was fixed prior to run 19 (Configuration No. 2) and the model was changed back to configuration No.

1 for run 21. This run verified that the mild flutter was indeed due to the model hatches (flutter was not encountered during this run) and was not characteristic of the fin design. After completion of tests on Configurations 2, 3 and 4, runs 29 and 30 were made to clear Configuration 1 beyond the flight envelope. A visual inspection of the model after run 30 uncovered minor structural damage in the area of the forward root fitting. This damage was probably sustained during run 29 while passing through the buffet region. A summary plot of test conditions may be found in figure 8.

A reduction in the upper and lower rudder actuator stiffnesses was tested as Configuration No. 2. Runs 15 through 20 were used to test Configuration No. 2. During these runs a buffet region was encountered similar to that encountered during tests on Configuration 1. Also mild flutter was encountered which again was attributable to the model hinge hatch. Configuration 2 results are presented on figure 9.

For Configuration No. 3 the actuator stiffnesses were again reduced (see Table III). This reduction resulted in a clear uncoupled lower rudder rotation mode (Configurations 2 and 3 exhibited highly coupled rudder rotation modes). Runs 22 through 25 were made in this configuration and all runs exhibited lower rudder buzz as 0.8 Mach number was approached. See figure 10 for Configuration 3 test conditions.

For Configuration No. 4 the lower rudder actuator stiffness was increased to the same level as Configuration 2 and the upper rudder

actuator stiffness was reduced to a level below that tested in Configuration 3 (see Table III). In this configuration a clear uncoupled upper rudder rotation mode was observed. Runs 26, 27 and 28 were made in this configuration and all runs exhibited upper rudder buzz as 0.8 Mach number was approached. See Figure 11 for Configuration 4 test conditions.

A summary of the maximum tunnel conditions tested with the fin in all configurations may be found in Table I.

Results of pre-tunnel checks and wind tunnel tests performed on the fin model permitted the following conclusions:

1. The fin model was a good dynamic representation of the design data as evidenced by pre-tunnel checks.
2. Wind tunnel tests on the fin indicated that a region of fin model buffet occurs as Mach 0.9 is approached.
3. When the stiffness of the flexures simulating the rudder actuators was reduced sufficiently to produce virtually uncoupled rudder rotation modes, rudder buzz resulted as Mach 0.8 was approached.

REFERENCES

1. F. Rauch and T. Foley, "Results of Dynamic Tests and Flutter Analyses Performed on .14 Scale Models of the Shuttle Wing and Fin," Grumman Aerospace Report NO LD-RS-11, November 18, 1974.

2. Manual on Aeroelasticity, Volume IV, AGARD.

3. C. L. Berthold, "Pretest Information for Component SSV Flutter Tests of 0.14-Scale Wing-Elevon (54-0) and Fin-Rudder (55-0) Models in the NASA-LRC 16-Foot Transonic Dynamics Tunnel (Tests OS6 and OS7)," Rockwell International Report SD74-SH-0148, July 5, 1974.

4. Langley Working Paper (LWP-799) - The Langley Transonic Dynamics Tunnel, September 23, 1969.

5. Drawings:

Drawing No.	Description
SS-S-00200	General Arrangement and Assembly
SS-S-00152	Installation LRC TDT
SS-S-00202	Skin Definition - Fin
SS-S-00203 (1-4)	Skin Definition - Rudder
SS-S-00204	Mount Assembly - Checkout
SS-S-00205	Fuselage Frame Assembly
SS-S-00206	Fuselage Shell and Frame Assembly
SS-S-00209 (1-2)	Shaker Assembly and Details
SS-S-00210	Fin Fitting and Flexures
SS-S-00214	Flexures and Fittings, Z_o = 661.8 and 760.1
SS-S-00215	Flexures and Fittings, Z_o = 610.1 and 697.3
SS-S-00217	Rudder Actuator Details
SS-S-00218	Fixture and Fittings (H.L. Inertia)
SS-S-00220	Vertical Tail - Lines and Geometry
SS-S-00221	Rib Arrangement

TABLE I. TEST SUMMARY

CONFIGURATION			RUN	MAX. TUNNEL CONDITIONS*				NOMINAL FREESTREAM TOTAL PRESSURE (PSF)	REMARKS
NO.	RUDDER FLEXURE THICKNESS (INCHES)**		NO.	MACH NO.	DYNAMIC PRESS. (PSF)	DENSITY (SLUGS/FT^3)	VELOCITY (FT/SEC)		
	LOWER RUDDER	UPPER RUDDER							
1	0.245	0.261	1	.906	65.4	.00064	451.3	100 & 200	
			2	---	--	--	--	---	Run Aborted-No Data
			3	.507	127.1	.00389	254.3	NA	Rudder Hatch
			4	.734	199.9	.00292	368.5	800	↓ Lifted
			5	.851	203.6	.00222	427.1	650	
			6	.244	16.1	.00207	124.1	---	Calibration Run-No Data
			7	.831	147.1	.00167	419.2	500	
			8	.888	140.0	.00139	447.3	450	
			9	.948	127.2	.00112	475.8	400	
			10	1.111	280.9	.00177	562.1	350	
			11	.737	281.2	.00395	375.7	NA	
			12	.741	200.4	.00282	375.6	850	
			13	.754	169.0	.00227	384.9	700	
			14	.784	150.3	.00187	399.7	600	
			21	.890	261.5	.00251	454.6	850	
			29	.956	302.5	.00260	480.7	900	
			30	.868	338.7	.00346	440.4	1100	
2	0.201	0.278	15	.851	94.0	.00099	434.2	300	
			16	1.003	156.2	.00124	500.8	400	
			17	.852	179.0	.00194	428.1	600	
			18	.792	209.4	.00262	398.6	750	
			19	.888	231.4	.00231	446.6	700	
			20	.843	294.0	.00320	427.0	1000	
3	0.142	0.163	22	.801	84.6	.00103	404.2	300	Buzz on Lower Rudder
			23	.792	120.9	.00150	400.0	450	
			24	.783	185.3	.00230	400.4	700	
			25	.777	265.3	.00332	397.8	1000	

TABLE I. TEST SUMMARY (Concluded)

CONFIGURATION			RUN	MAX. TUNNEL CONDITIONS*				NOMINAL FREESTREAM TOTAL PRESSURE (PSF)	REMARKS
NO.	RUDDER FLEXURE THICKNESS (INCHES)**			MACH NO.	DYNAMIC PRESS. (PSF)	DENSITY (SLUGS/FT^3)	VELOCITY (FT/SEC)		
	LOWER RUDDER	UPPER RUDDER	NO.						
4	0.201	0.130	26	.839	90.9	.00101	422.7	300	Buzz on Lower Rudder
↓	↓	↓	27	.804	150.8	.00181	407.2	550	↓
			28	.803	218.9	.00261	408.0	800	

* NASA-supplied, based on measured tunnel parameters.

** Each rudder had 4 flexures, each flexure was 1.75 inches long by 0.5 inch wide with a thickness as listed.

TABLE II. MODEL DIMENSIONAL DATA

MODEL COMPONENT: BODY - B_{26}

GENERAL DESCRIPTION: Configuration 140A/B orbiter fuselage

NOTE: B_{26} is identical to B_{24} except underside of fuselage has refaired to accept W_{116}.

MODEL SCALE: 0.140 MODEL DRAWING: SS-A00147, Release 12

DRAWING NUMBER: VL70-000143B, -000200, -000205, -006089, -000145
VL70-000140A, -000140B

DIMENSIONS:	FULL SCALE	MODEL SCALE
Length (OML: Fwd Sta X_o = 235), In.	1293.3	181.062
Length (IML: Fwd Sta X_o = 238), In.	1290.3	180.642
Max Width (@ X_o = 1528.3), In.	264.00	36.96
Max Depth (@ X = 1464), In.	250.00	35.00
Fineness Ratio	0.26357	0.26357
Area - Ft^2		
Max. Cross-Sectional	340.88	6.68

TABLE II. MODEL DIMENSIONAL DATA (Continued)

MODEL COMPONENT: OMS/RCS PODS - M_7

GENERAL DESCRIPTION: Configuration 140A/B Orbiter OMS/RCS pods.

MODEL SCALE: 0.140 MODEL DRAWING: SS-A00147, Release 12

DRAWING NUMBER: VL70-000145

DIMENSIONS:	FULL SCALE	MODEL SCALE
Length (OMS Fwd Sta X_o = 1233.0), In.	327.000	45.78
Max Width (@ X_o = 1450.0), In.	94.500	13.230
Max Depth (@ X_o = 1493.0), In.	109.000	15.25

TABLE II. MODEL DIMENSIONAL DATA (Continued)

MODEL COMPONENT: RUDDER - R_5

GENERAL DESCRIPTION: Configuration 140 C/D Orbiter rudder (identical to configuration 140A/B rudder)

MODEL SCALE: 0.140

DRAWING NUMBER: VL70-000146B, VL70-000095

DIMENSIONS:	FULL SCALE	MODEL SCALE
Area - Ft^2	100.15	1.963
Span (equivalent), In.	201.00	28.14
Inb'd equivalent chord, In.	91.585	12.822
Outb'd equivalent chord, in.	50.833	7.117
Ratio movable surface chord/ total surface chord		
At Inb'd equiv. chord	0.400	0.400
At Outb'd equiv. chord	0.400	0.400
Sweep Back Angles, degrees		
Leading Edge	34.83	34.83
Trailing Edge	26.25	26.25
Hingeline	34.83	34.83
Area Moment (Product of area & $\bar{c}$), Ft^3	610.92	1.676
Mean Aerodynamic Chord	73.2	10.248

TABLE II. MODEL DIMENSIONAL DATA (Concluded)

MODEL COMPONENT: VERTICAL - V8

GENERAL DESCRIPTION: Configuration 140 C/D Orbiter Vertical Tail (Identical to configuration 140 A/B Vertical Tail).

MODEL SCALE: 0.140

DRAWING NUMBER: VL70-000140C, VL70-000146B

DIMENSIONS:	FULL SCALE	MODEL SCALE
TOTAL DATA		
Area (Theo) - Ft^2		
Planform	413.253	8.100
Span (Theo) - In.	315.72	44.201
Aspect Ratio	1.675	1.675
Rate of Taper	0.507	0.507
Taper Ratio	0.404	0.404
Sweep-Back Angles, Degrees		
Leading Edge	45.000	45.000
Trailing Edge	26.25	26.25
0.25 Element Line	41.13	41.13
Chords:		
Root (Theo) WP	268.50	37.590
Tip (Theo) WP	108.47	15.186
MAC	199.81	27.973
Fus. Sta. of .25 MAC	1463.25	204.869
W.P. of .25 MAC	635.52	88.973
B.L. of .25 MAC	0.00	0.00
Airfoil Section		
Leading Wedge Angle - Deg.	10.00	10.00
Trailing Wedge Angle - Deg.	14.92	14.92
Leading Edge Radius	2.00	0.28
Void Area	13.17	0.258
Blanketed Area	0.00	0.00

TABLE III. CONFIGURATION DESCRIPTION AND FREQUENCY SUMMARY

CONF. NO.	CONFIGURATION DESCRIPTION	MEASURED FREQUENCIES (HZ)						
		1	2	3	4	5	6	7
1	2 sets of 2 upper flexures - thickness=.261, width=.50 2 sets of 2 lower flexures - thickness=.245, width=.50	10.2	24.5	42.3	44.8	77.0	101.0	107.0
2	2 sets of 2 upper flexures - thickness=.218, width=.50 2 sets of 2 lower flexures - thickness=.201, width=.50	10.0	24.5	41.0	44.0	64.5	97.2	102.8
3	2 sets of 2 upper flexures - thickness=.163, width=.50 2 sets of 2 lower flexures - thickness=.142, width=.50	10.0	24.5	35.2	42.2	55.0	-	-
4	2 sets of 2 upper flexures - thickness=.130, width=.50 2 sets of 2 lower flexures - thickness=.201, width=.50	9.8	24.5	37.6	41.5	55.5	103.2	-

NOTE: Flexures are made of steel and are configured as 90° cross flexures.

TABLE IV. MEASURED MODEL ROOT FLEXIBILITIES

Forward Root Fitting Flexibilities

AXIS	DESIGN VALUE (IN/LB)	MEASURED VALUE (IN/LB)
Y	0.33×10^{-5}	0.33×10^{-5}
Z	1.99×10^{-5}	1.85×10^{-5}

Aft Root Fitting Flexibilities*

AXIS	DESIGN VALUE (IN/LB)	MEASURED VALUE (IN/LB)
Y	11.74×10^{-5}	12.3×10^{-5}
Z	1.96×10^{-5}	1.92×10^{-5}

* One side only (fitting symmetrical)

TABLE V. PANEL MASS, INERTIA, AND C.G. VALUES

a. Vertical Tail

FIN WITH RUDDERS						
PANEL NO.	WEIGHT (LBS)	Z'_{CG} (IN)	X'_{CG} (IN)	$I_{Z'CG}$ (LB-IN^2)	$I_{X'CG}$ (LB-IN^2)	$I_{Y'CG}$ (LB-IN^2)
1	3.05	4.50	-4.60	79.98	NA	NA
2	2.13	14.83	-0.70	46.12	↓	↓
3	3.21	20.63	1.70	64.52		
4	1.90	25.59	1.44	50.12		
5	2.75	30.59	1.70	40.53		
6	2.29	36.07	1.50	30.13		
7	0.96	40.48	1.40	14.13		
8	0.85	44.18	1.50	10.93		
9	1.44	47.18	1.30	10.13		
10	.63	50.18	1.70	5.87		
11	.18	55.18	3.40	1.07	▼	▼
TOTAL CALCULATED VALUE	19.38	26.44	0.36	453.0	3835.0	4234
MEASURED VALUE*	20.85	25.10	-0.10	487.8	4506.0	5193

*Actual measured values included, fuselage root fittings and external strain gage wire. Items at right were mathematically removed from the measured values to obtain "corrected" values.

ITEM	W (LBS)	X'_{CG} (IN)	Z'_{CG} (IN)
Fitting	0.33	-10.0	-7.5
Fitting	0.21	0.0	2.5
Wire	0.20	0.0	2.5

CALCULATED VALUES FOR FIN WITHOUT RUDDERS					
PANEL NO.	WEIGHT (LBS)	Z'_{CG} (IN)	X'_{CG} (IN)	$I_{Z'CG}$ (LB-IN^2)	$I_{X'CG}$ (LB-IN^2)
1	3.05	4.50	-4.60	79.98	144.48
2	2.13	14.83	-0.70	46.12	47.17
3	2.52	20.57	0.75	51.07	52.50
4	1.35	25.59	-0.76	23.87	24.66
5	1.98	30.61	0.28	20.99	21.15
6	1.64	36.25	0.04	14.43	14.43
7	0.67	40.51	-0.36	6.12	6.12
8	0.56	44.18	-0.22	4.88	4.91
9	1.09	47.17	0.43	5.53	5.73
10	0.40	49.96	0.04	2.31	2.31
11	0.18	55.18	3.40	1.07	3.13
TOTALS	15.58	24.73	-0.85	315.3	---

Refer to Figure 7 for definition of panels.

TABLE V. PANEL MASS, INERTIA, AND C.G. VALUES (Concluded)

b. Rudders

UPPER RUDDER						
PANEL NO.	WEIGHT (LBS)	Z'_{CG} (IN)	X'_{CG} (IN)	$I_{Z'_{CG}}$ (LB-IN^2)	$I_{X'_{CG}}$ (LB-IN^2)	I_{H_L} (LB-IN^2)
6R	0.65	35.59	5.20	3.33	20.84	NA
7R	0.29	40.42	5.40	1.23	9.81	↓
8R	0.29	44.18	4.90	1.07	7.93	
9R	0.35	47.22	4.00	1.23	6.83	
10R	0.22	50.58	4.68	0.45	5.37	↓
TOTAL CALCULATED VALUE	1.80	41.87	4.89	--	--	24.0
MEASURED VALUE	1.81	41.70	5.05	53.3	9.4	22.2

LOWER RUDDER						
PANEL NO.	WEIGHT (LBS)	Z'_{CG} (IN)	X'_{CG} (IN)	$I_{Z'_{CG}}$ (LB-IN^2)	$I_{X'_{CG}}$ (LB-IN^2)	I_{H_L} (LB-IN^2)
3R	0.68	20.87	5.20	2.80	21.31	NA
4R	0.55	25.59	6.84	3.60	29.41	↓
5R	0.73	30.53	5.40	5.07	27.32	↓
TOTAL CALCULATED VALUE	1.96	25.86	5.73	--	---	33.50
MEASURED VALUE	2.02	25.80	5.25	37.50	14.70	34.40

Refer to Figure 7 for definition of panels.

TABLE VI. MODAL ORTHOGONALITY CHECKS AND GENERALIZED MASS FOR FIN WITH STIFF ACTUATORS

MODE	1	2	3	4	5	6	7
1	1.000	.0027	.0237	.0019	.0031	.0006	.0003
2	———	1.000	.0107	.0209	.0042	.0256	.0092
3	———	———	1.000	.0002	.0108	.0003	.000007
4	———	———	———	1.000	.0088	.0018	.0082
5	———	———	———	———	1.000	.1706	.0048
6	———	———	———	———	———	1.000	.1269
7	———	———	———	———	———	———	1.000
FREQ. (HZ)	10.15	42.30	44.80	71.00	101.00	107.00	135.00
CALCULATED GENERALIZED MASS (LBS.)	3.367	2.457	1.934	0.8626	.6085	0.9804	0.3698

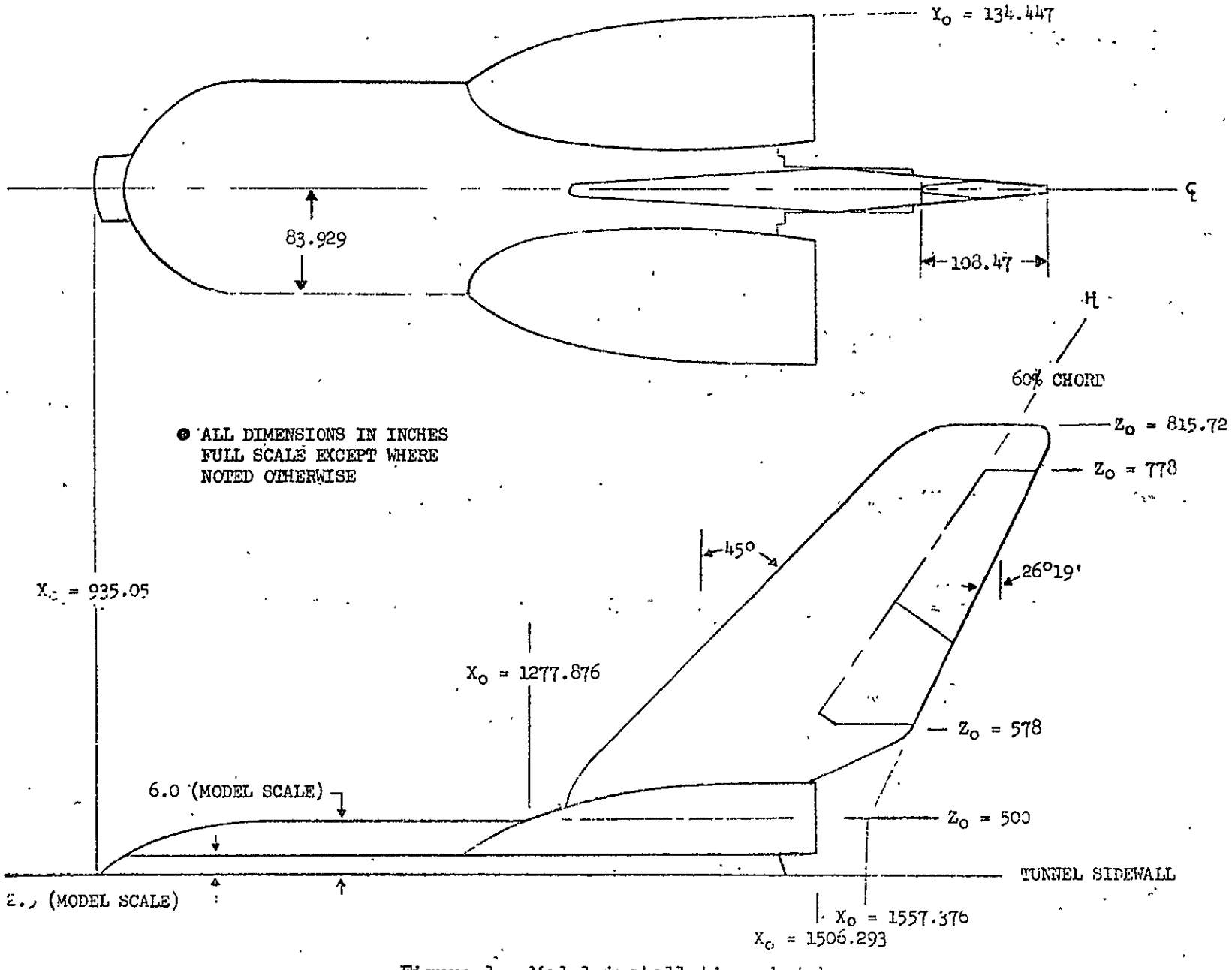

Figure 1. Model installation sketch.

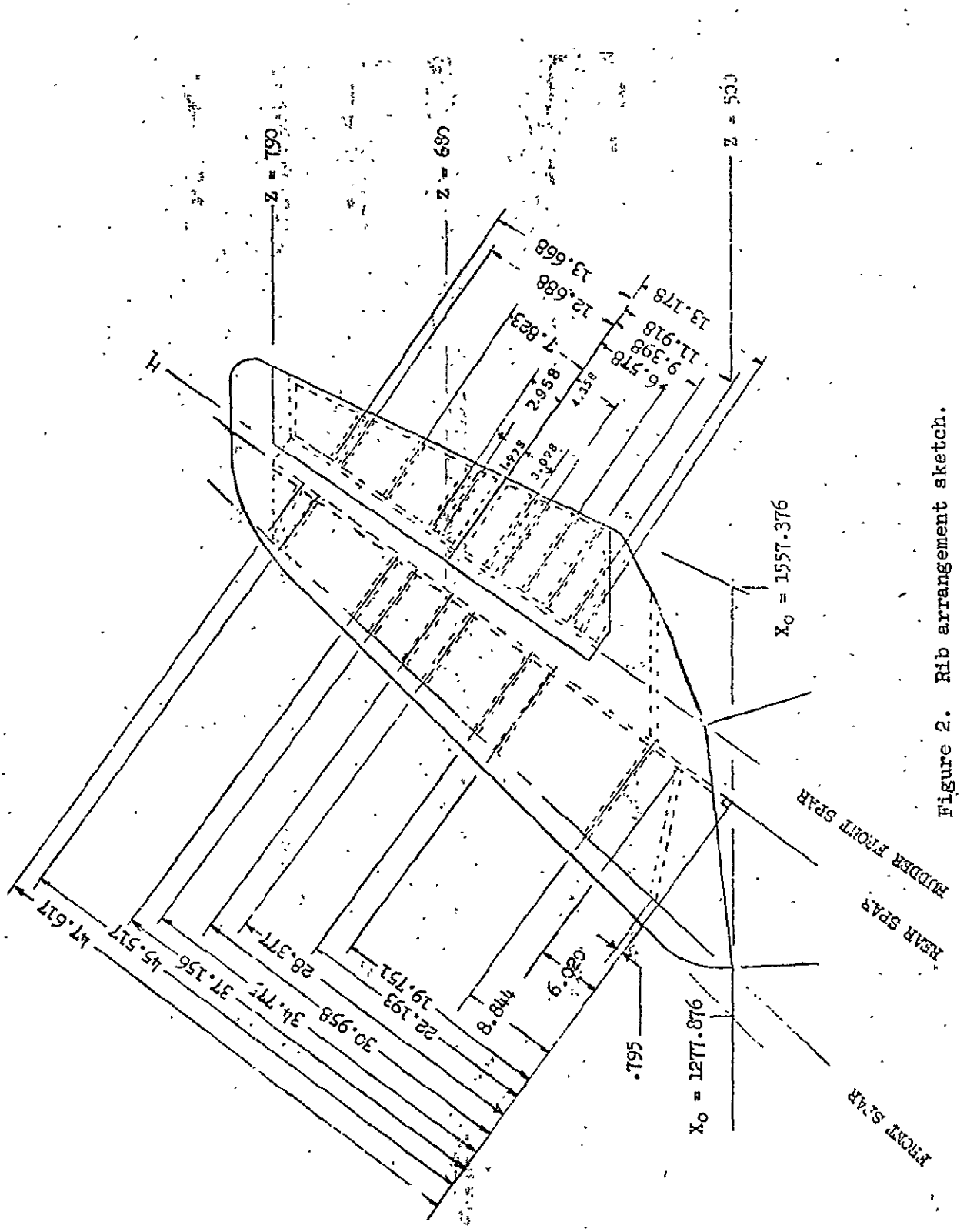

Figure 2. Rib arrangement sketch.

a. Vertical Tail

Figure 3. Model photographs.

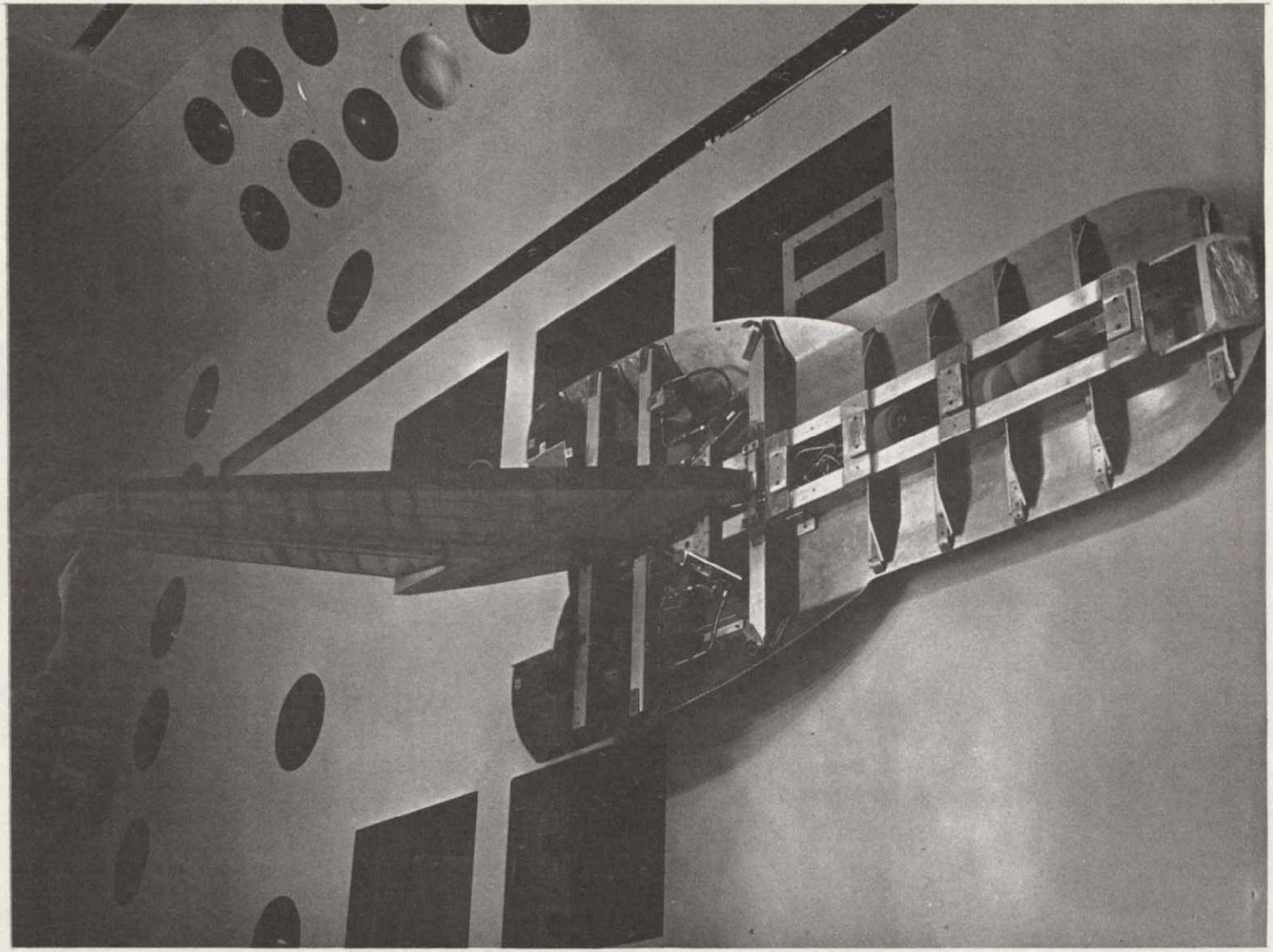

b. Fuselage Structure with Skin Removed
Figure 3. Continued.

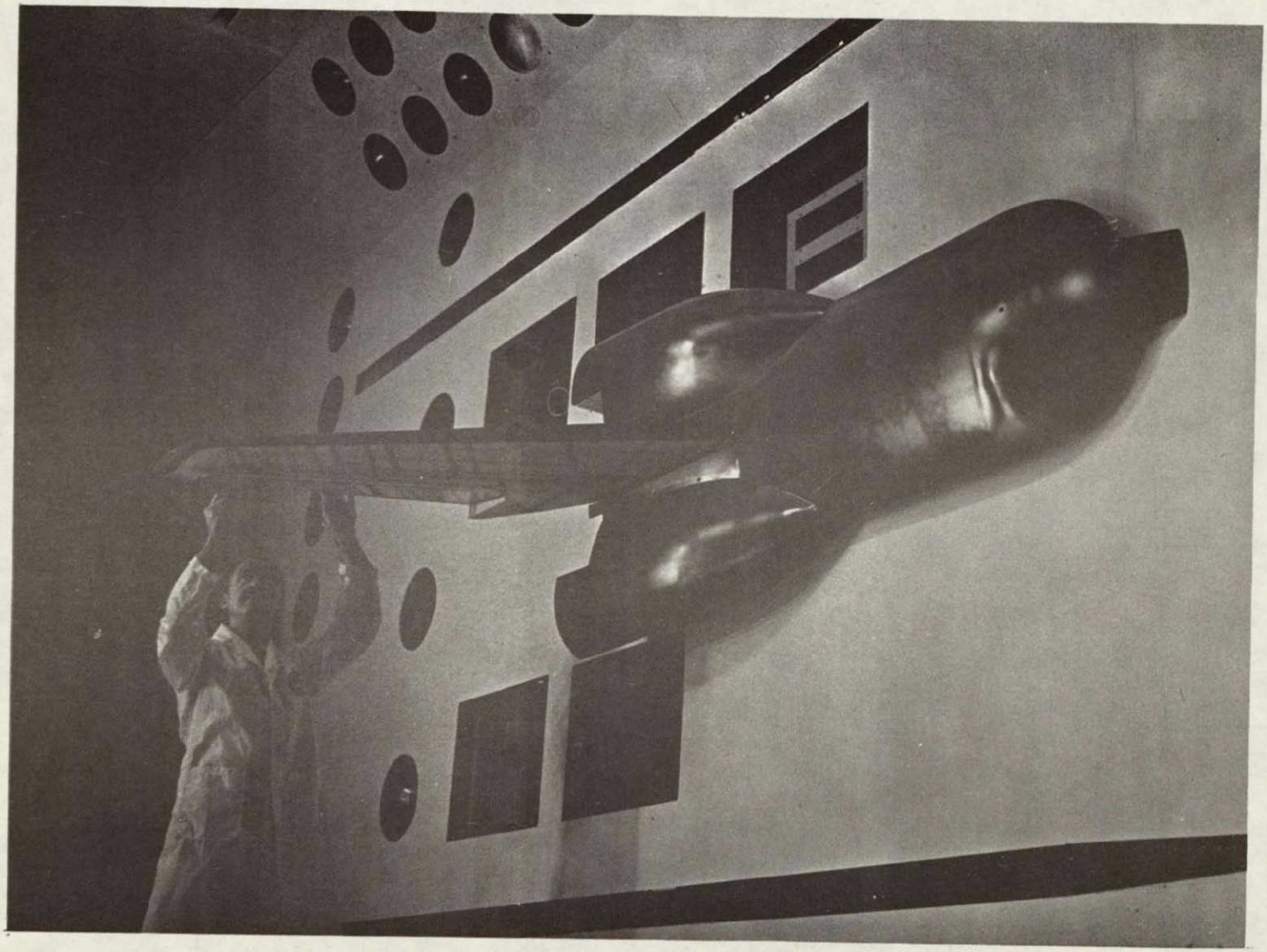

c. Complete Model Assembly Mounted in the LaRC 16 TDT
Figure 3. Concluded.

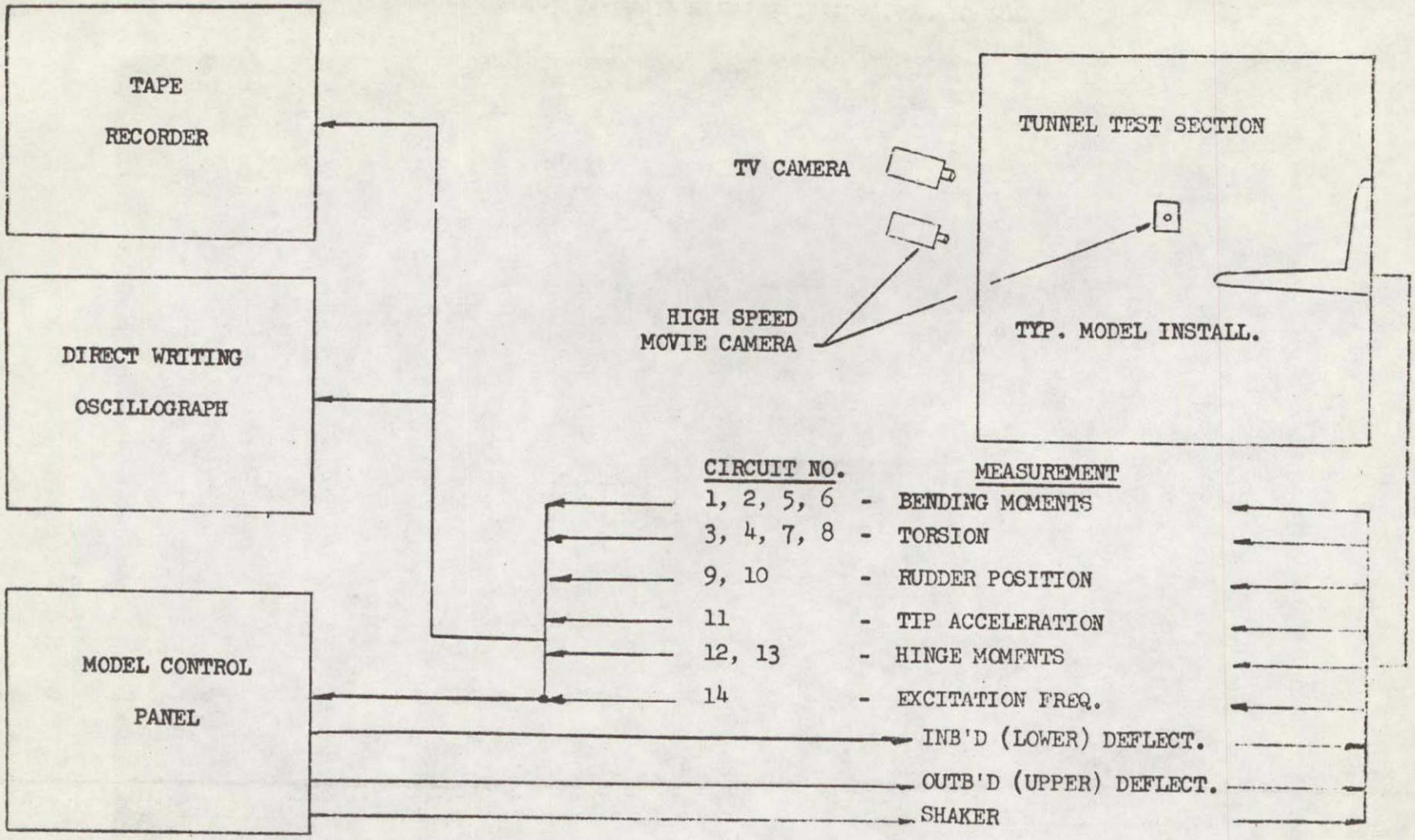

Figure 4. Model instrumentation diagram.

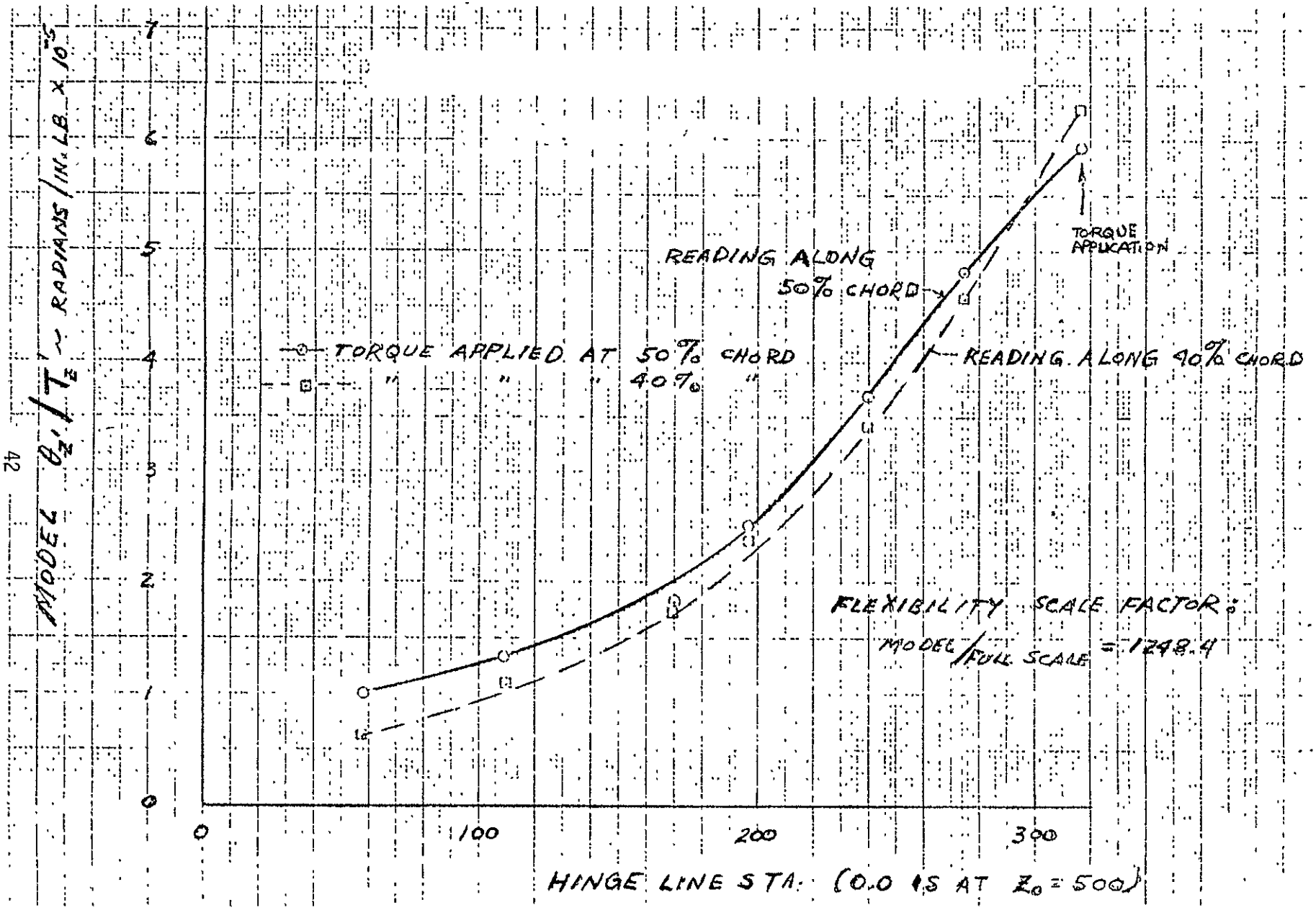

Figure 6. Torsional flexibility.

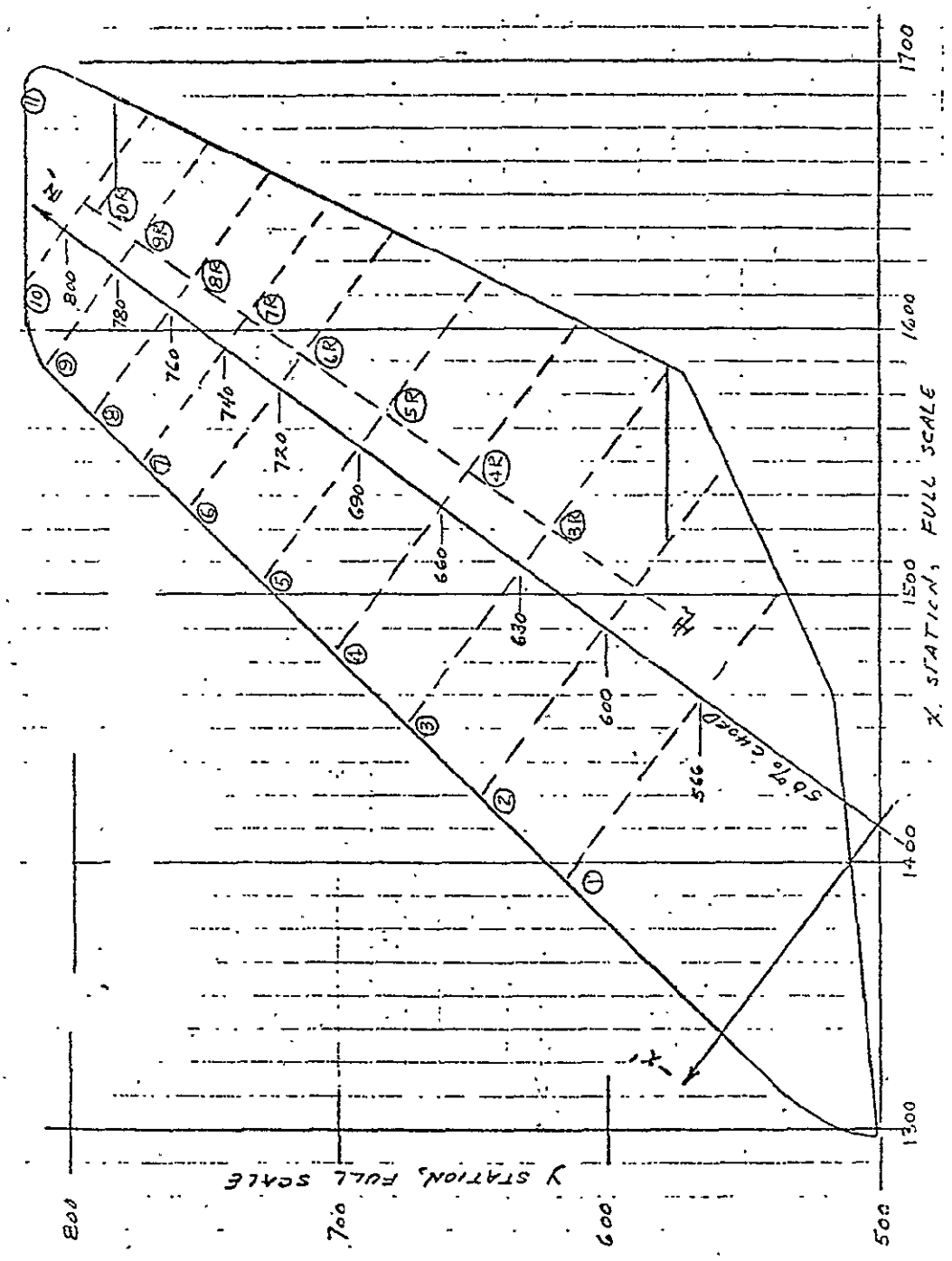

Figure 7. Panel definition for mass and inertia measurements.

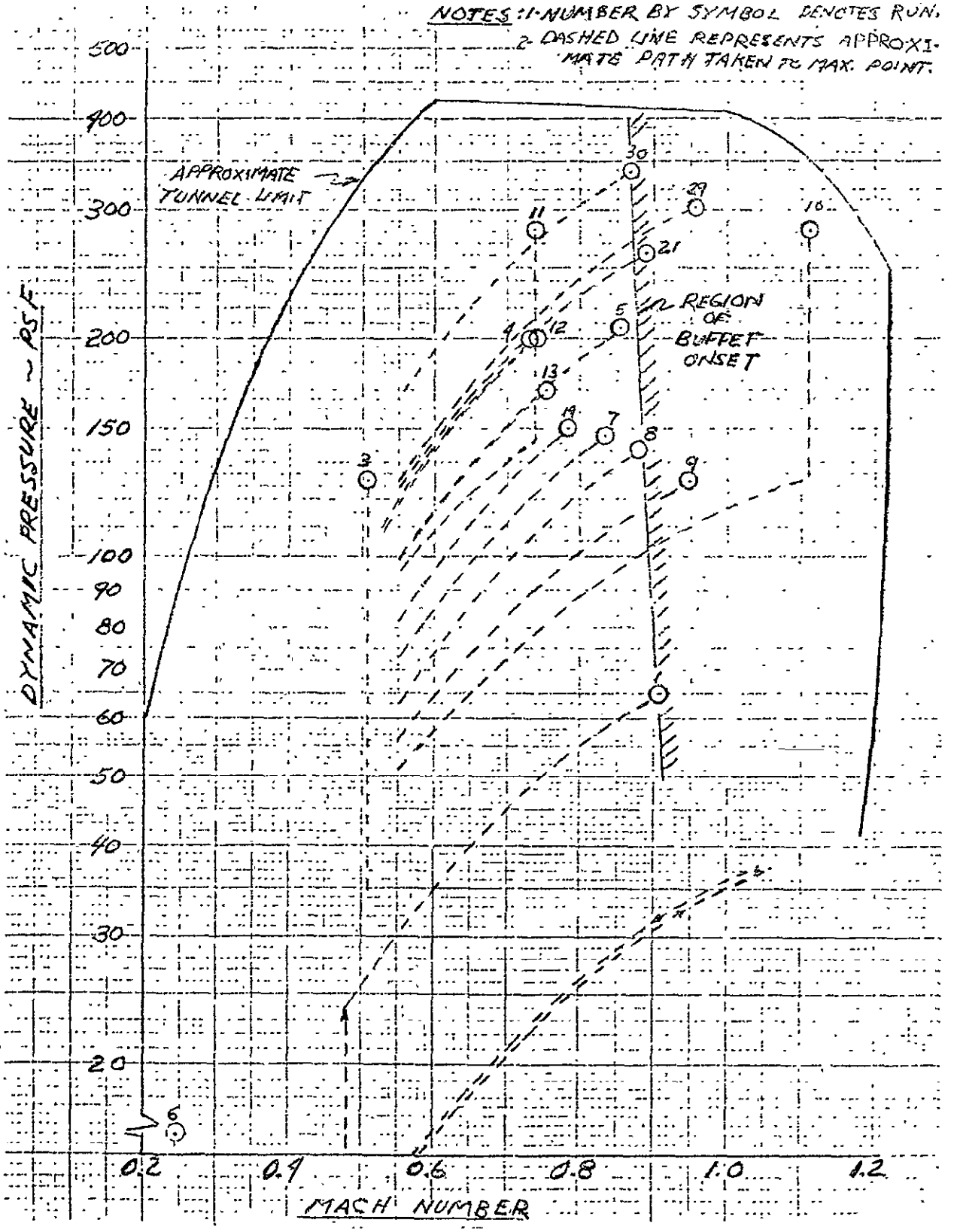

Figure 8. Flutter boundary for configuration No. 1.

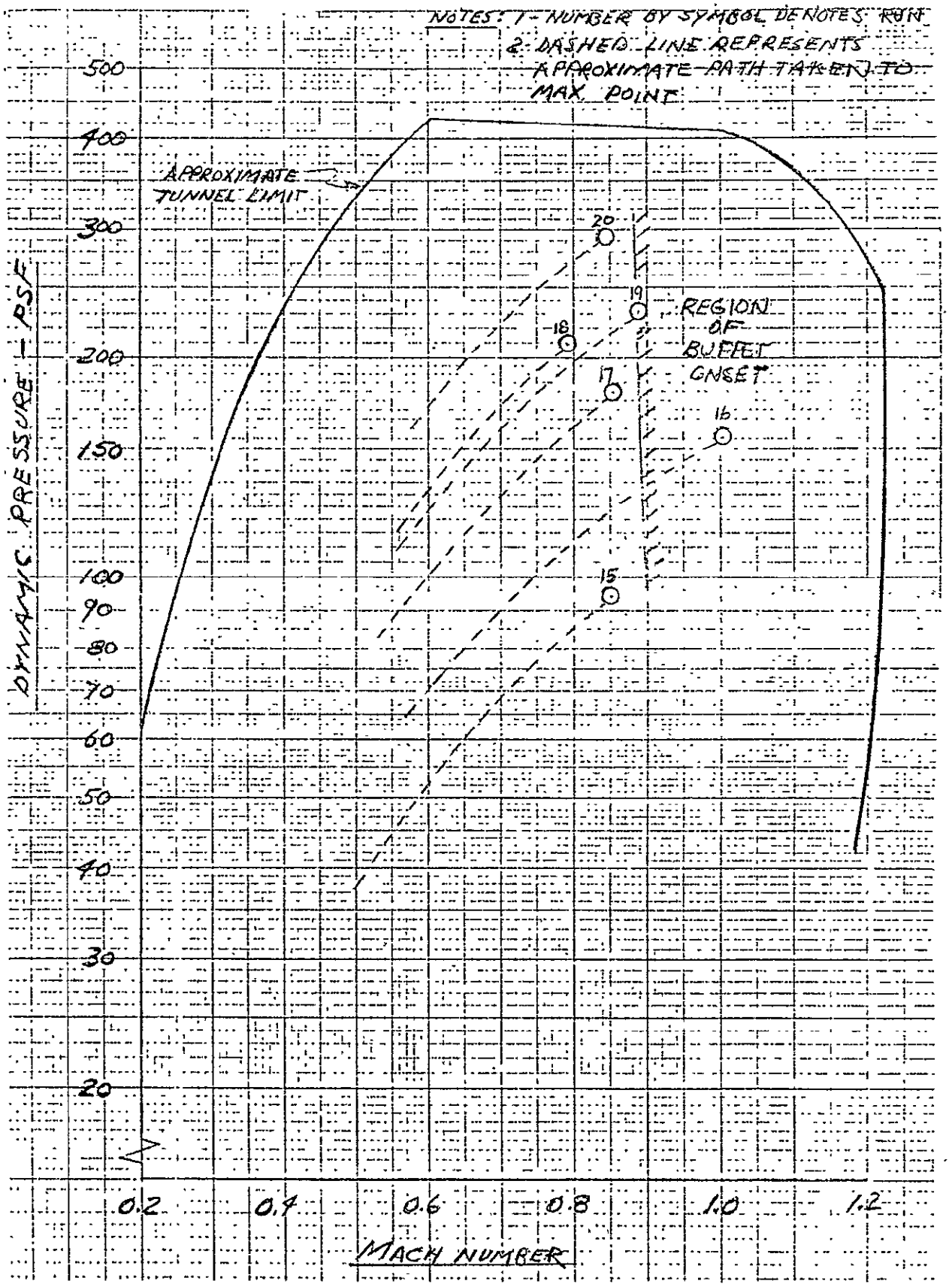

Figure 9. Flutter boundary for configuration No. 2.

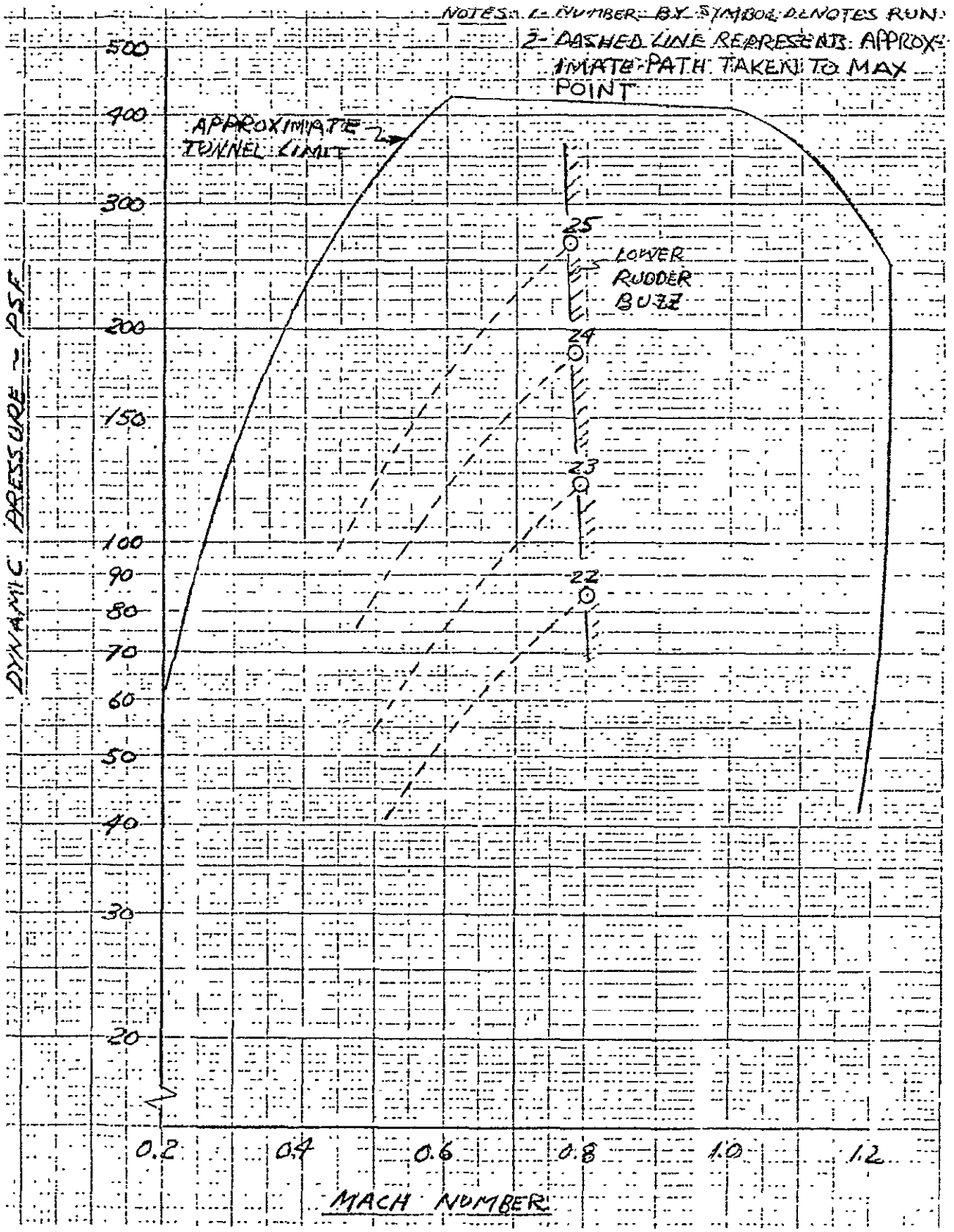

Figure 10. Flutter boundary for configuratio No. 3.

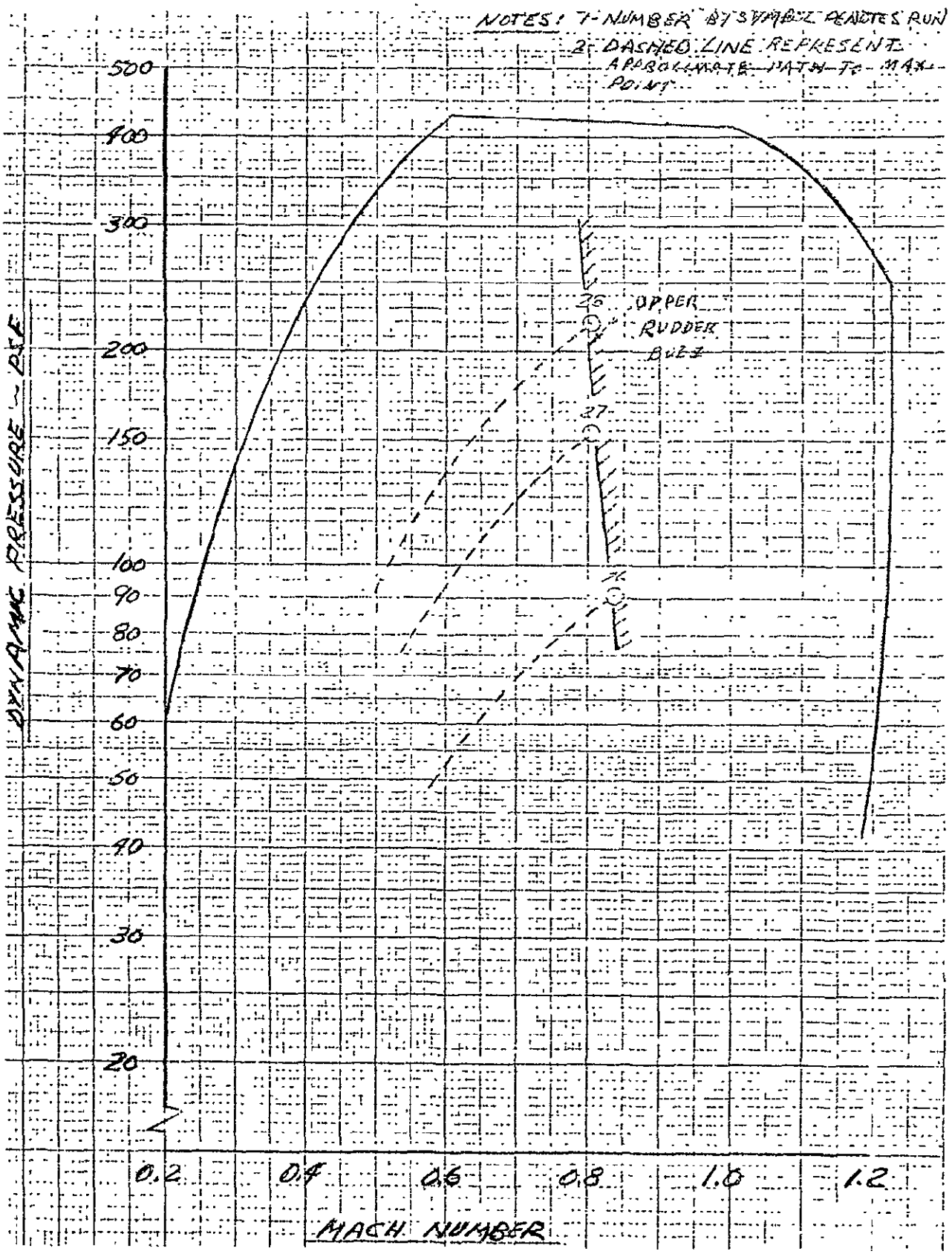

Figure 11. Flutter boundary for configuration No. 4.

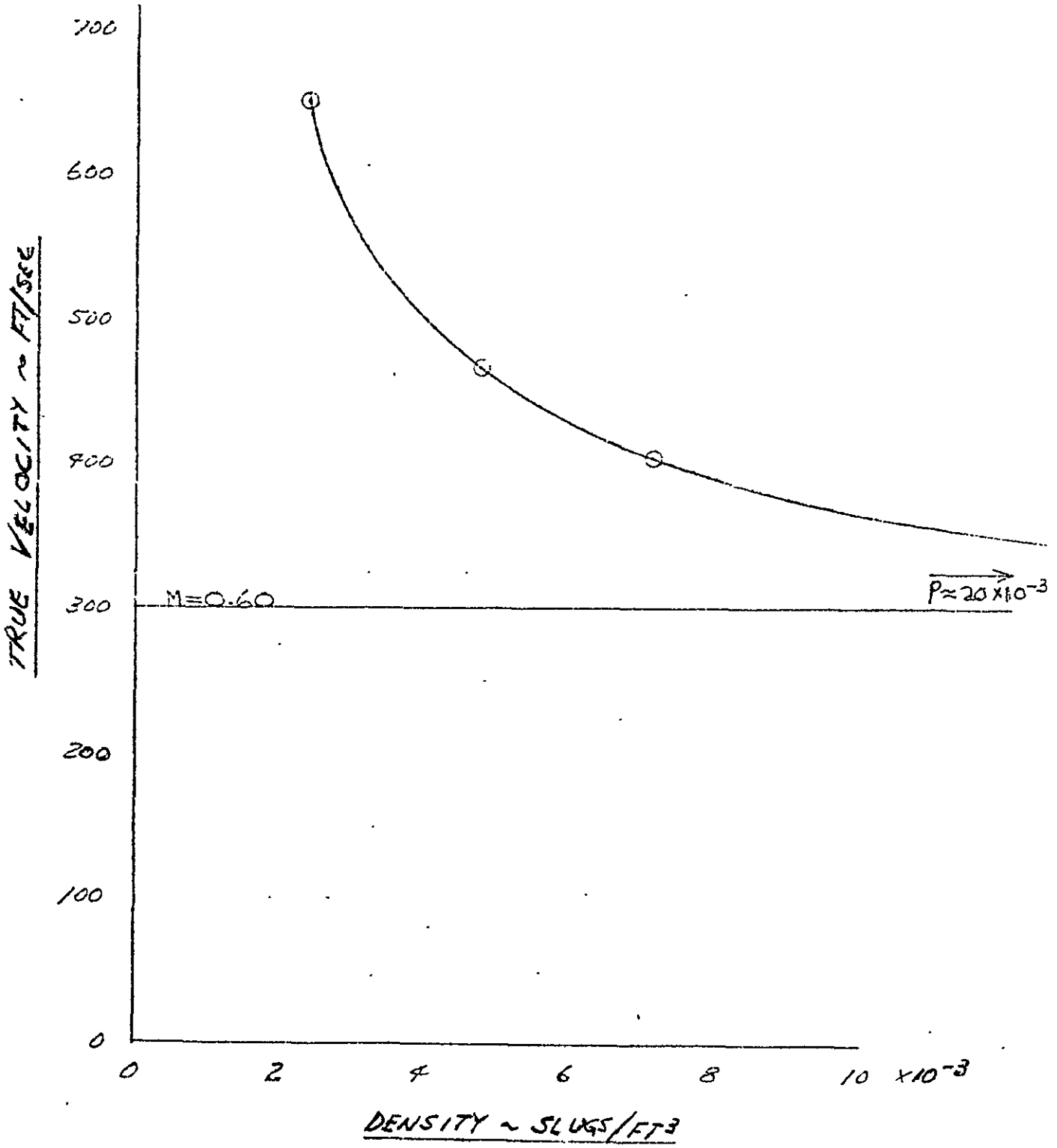

Figure 12. True velocity versus density at Mach .6.

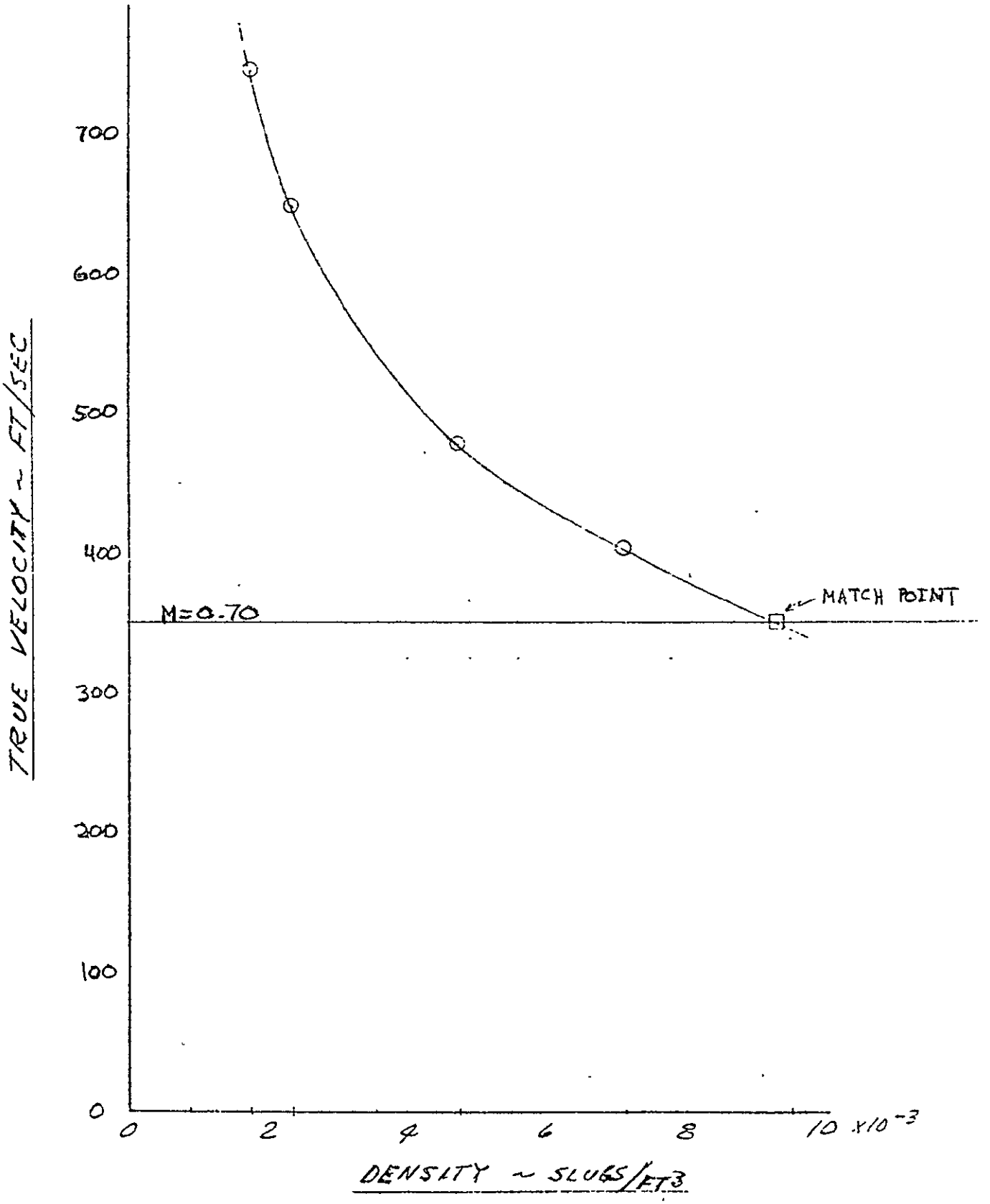

Figure 13. True velocity versus density at Mach .7.

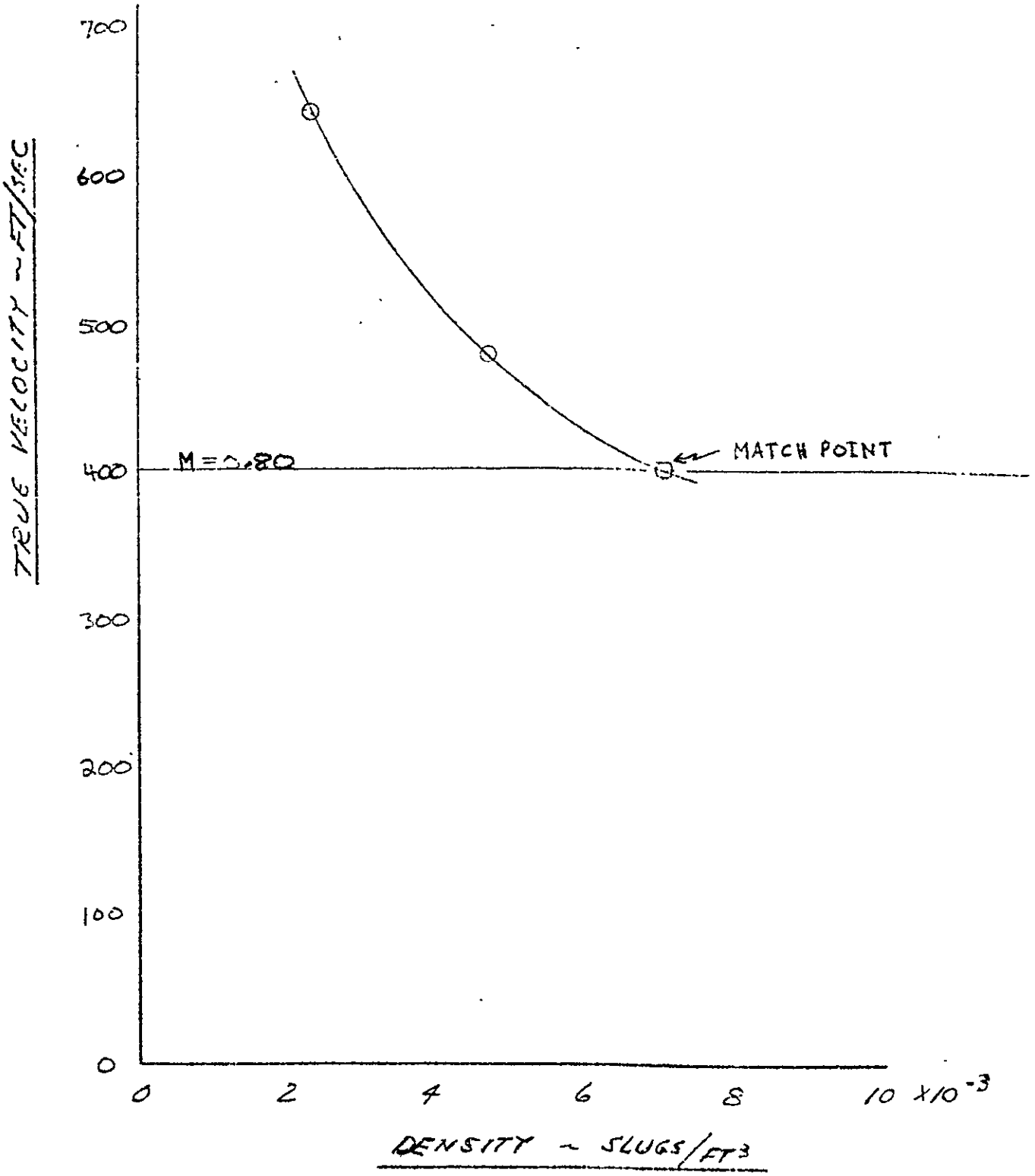

Figure 14. True velocity versus density at Mach .8.

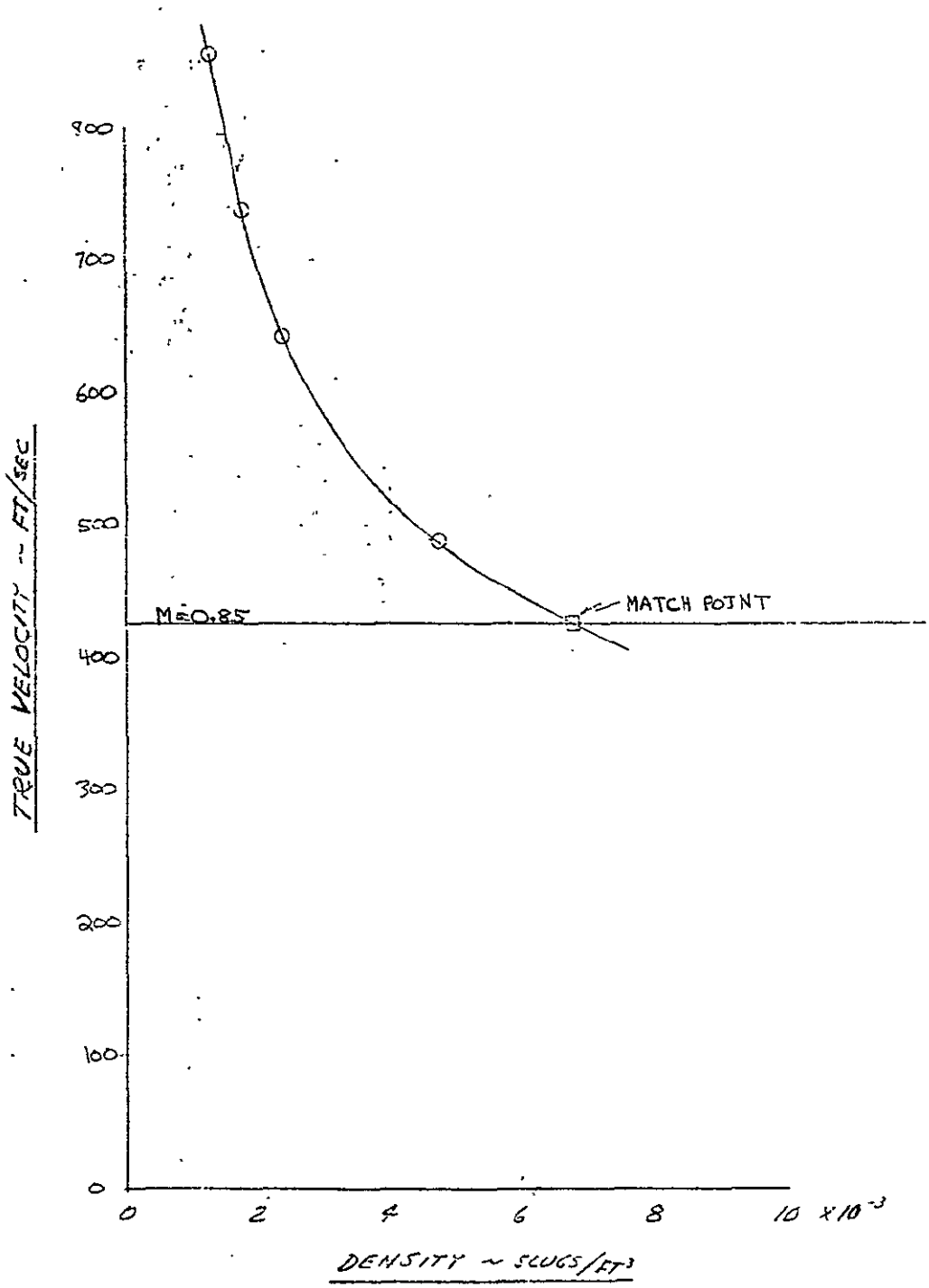

Figure 15. True velocity versus density at Mach .85.

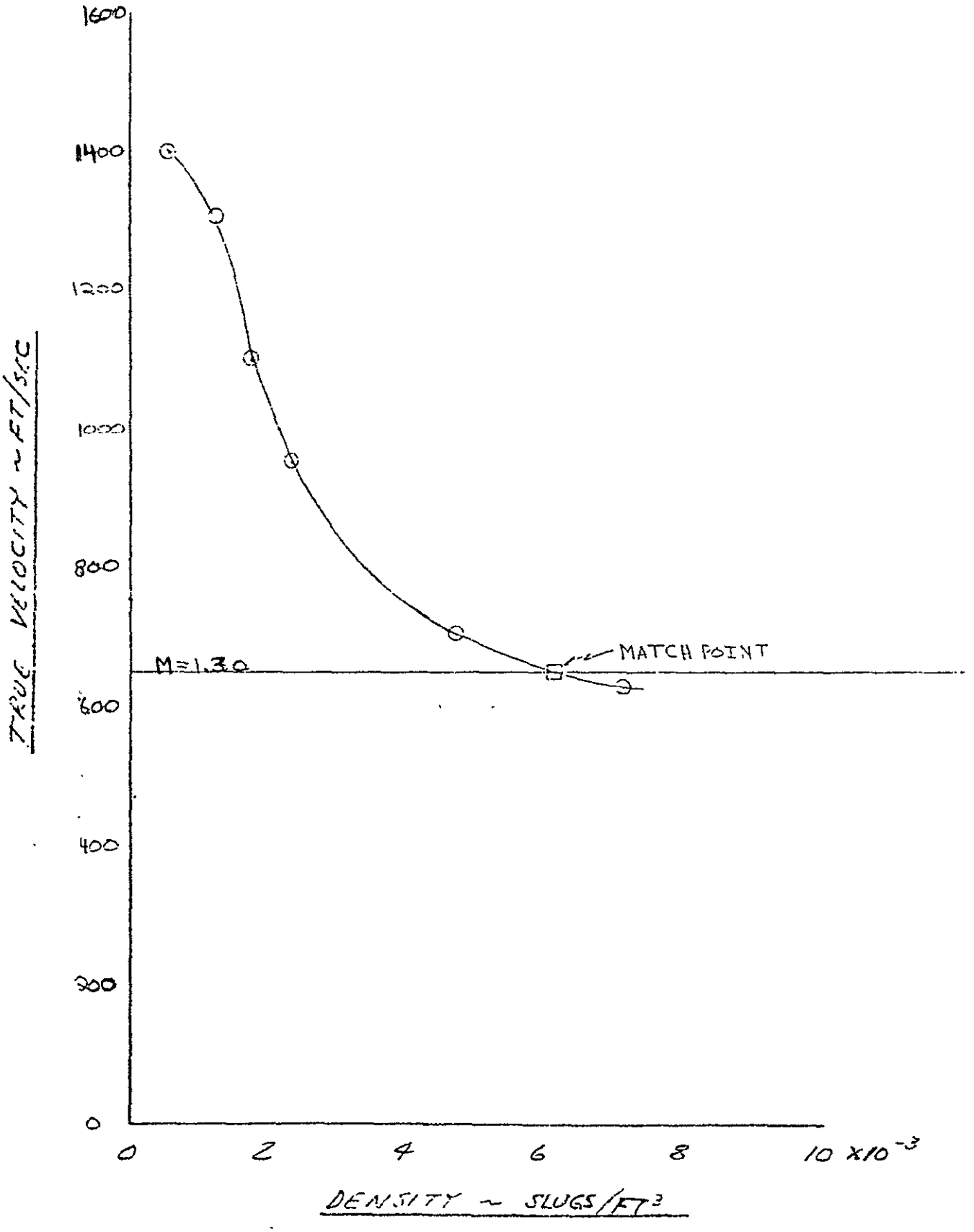

Figure 16. True velocity versus density at Mach 1.3.

Figure 17. Damping versus Mach number.

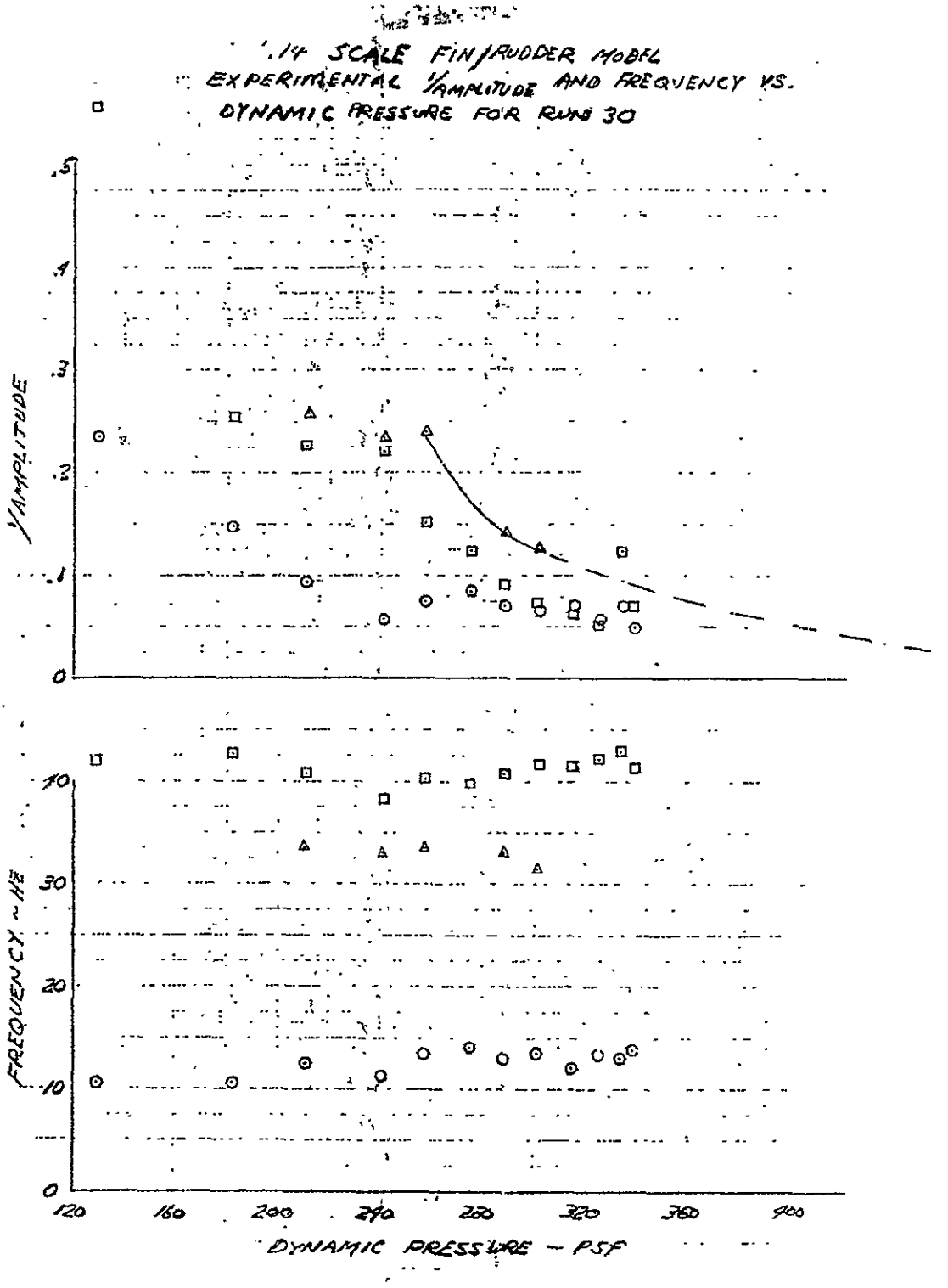

Figure 18. Inverse of amplitude and frequency versus dynamic pressure.